HHS Public Access

Author manuscript

Dev Dyn. Author manuscript; available in PMC 2017 May 17.

Published in final edited form as:

Dev Dyn. 2016 January ; 245(1): 22–33. doi:10.1002/dvdy.24355.

A Kupffer's vesicle size threshold for robust left-right patterning of the zebrafish embryo

Jason J. Gokey, **Yongchang Ji**, **Hwee Goon Tay**, **Bridget Litts**, and **Jeffrey D. Amack***

Department of Cell and Developmental Biology, State University of New York, Upstate Medical University, Syracuse, NY, USA

Abstract

Background—Motile cilia in the 'organ of asymmetry' create directional fluid flows that are vital for left-right (LR) asymmetric patterning of vertebrate embryos. Organ function often depends on tightly regulated organ size control, but the role of organ of asymmetry size in LR patterning has remained unknown. Observations of the organ of asymmetry in the zebrafish — called Kupffer's vesicle (KV)—have suggested significant variations in KV size in wild-type embryos, raising questions about the impact of KV organ size on LR patterning.

Results—To understand the relationship between organ of asymmetry size and its function, we characterized variations in KV at several developmental stages and in several different zebrafish strains. We found that the number of KV cilia and the size of the KV lumen were highly variable, whereas the length of KV cilia showed less variation. These variabilities were similar among different genetic backgrounds. By specifically modulating KV size and analyzing individual embryos, we identified a size threshold that is necessary for KV function.

Conclusions—Together these results indicate the KV organ of asymmetry size is not tightly controlled during development, but rather must only exceed a threshold to direct robust LR patterning of the zebrafish embryo.

Keywords

Left-right patterning; Cilia; Congenital disease; Organ size control; Developmental noise

Introduction

Establishing the left-right (LR) body axis in the vertebrate embryo has been an interesting and enigmatic topic of developmental biology for many years. Clinical observations and animal models have shown that alterations in LR development result in congenital malformations of the gastrointestinal and cardiovascular systems (Ramsdell, 2005; Sutherland and Ware, 2009). In the 1970s, identification of cilia defects in Kartagener syndrome patients with reversed LR asymmetry (Afzelius, 1976) suggested a link between cilia motility and LR axis determination. In the 1990s, the cup-shaped ventral node in the mouse embryo was found to contain motile cilia that create a directional right-to-left fluid flow that is necessary for establishing LR asymmetry (Nonaka et al., 2002; Nonaka et al.,

*Author for correspondence: Jeffrey D. Amack, amackj@upstate.edu, Phone: 315.464.8507.

1998). Asymmetric fluid flows trigger Ca^{2+} signals in neighboring cells and a conserved Nodal (TGFβ family) signaling cascade in left lateral plate mesoderm that is thought to provide LR patterning information for the developing heart and gut. Ciliated organs that function analogous to the murine ventral node during LR development have been identified in other vertebrates, including the gastroceol roof plate (GRP) in frog (Schweickert et al., 2007) and Kupffer's vesicle (KV) in zebrafish (Essner et al., 2005; Kramer-Zucker et al., 2005) and medaka (Hojo et al., 2007). We refer to these structures as the ciliated 'organ of asymmetry'. However, exactly how these ciliated organs generate and transmit LR signals remains unclear.

Kupffer's vesicle (KV) in the zebrafish embryo has been an important model system for investigating the role of cilia in LR development. In contrast to other vertebrate models, the precursor cells that give rise to the ciliated KV have been clearly defined and can be tracked and manipulated during development. These progenitor cells, called dorsal forerunner cells (DFCs), are specified at the dorsal margin of the shield stage embryo approximately 5 hours post-fertilization (hpf) (Cooper and D'Amico, 1996; Oteiza et al., 2008). The initial group of ~20 DFCs migrate ahead of the dorsal margin and proliferate during epiboly stages. DFCs then cluster and undergo a mesenchymal-to-epithelial transition to differentiate into KV cells by 10 hpf in the tailbud. Epithelial KV cells create a fluid filled lumen that rapidly expands during early somite stages. At the same time, a single cilium forms and elongates from the apical surface of each KV cell to extend into the lumen. Between the 4–6 somite stages (11–12 hpf), regional cell shape changes, which we refer to as 'KV remodeling,' create a biased distribution of cilia in the dorsoanterior region of KV that drive strong leftward flow across the anterior pole of KV (Wang et al., 2012). Similar to the mouse ventral node, cilia-powered flows in KV are necessary to establish left-sided expression of the *Nodal*-related gene *southpaw* (*spaw*) in the lateral plate mesoderm at the 10 somite stage (Long et al., 2003) and subsequent asymmetric development of visceral organs (Essner et al., 2005; Kramer-Zucker et al., 2005; Long et al., 2003). How flow activates *spaw* is still contested, but recent work suggests intraciliary calcium fluxes initiate asymmetric calcium signaling on the left side of KV that relays LR information to the lateral plate mesoderm (Yuan et al., 2015).

In general, organ size control is a tightly regulated process during development and deviations in size often compromise organ function (Metcalf, 1963, 1964; Tumaneng et al., 2012). However, the relationship between size of the vertebrate organ of asymmetry and its function has remained unclear. It is plausible that size would impact fluid flow dynamics (Cartwright et al., 2004; Sampaio et al., 2014; Smith et al., 2012) that are essential for LR patterning. However, organ of asymmetry size varies greatly between vertebrate species (Amack, 2014; Blum et al., 2009; Lee and Anderson, 2008; Nakamura and Hamada, 2012), which raises the question of whether constructing a ciliated organ of a specific size is critical for generating LR signals. In the mouse embryo, the ventral node contains between 200–300 cilia, but analysis of cilia mutants revealed that only two motile cilia are required to generate LR asymmetry (Shinohara et al., 2012). In zebrafish, mathematical modeling simulations have predicted approximately 30 cilia are necessary in KV for LR patterning (Sampaio, 2014). However, a wide range of values for KV size and cilia reported in the literature has made it difficult to draw connections between KV form and function. To investigate the role

of ciliated organ size in LR patterning, we systematically quantified variations in KVs from several zebrafish strains and characterized the relationship between KV size and cilia formation. We report significant variabilities in KV development and a modest correlation between the number of ciliated cells and KV size. By modulating KV size and analyzing single embryos, we identified a minimum threshold for KV organ size needed to establish robust LR asymmetry.

Results

Kupffer's Vesicle exhibits significant variabilities during development in wild-type populations

During our investigations of KV development, we have noticed significant variations in KV organ size. For example, the number of KV cilia—which reflects the number of KV cells since each cell is monociliated—was as few as 31 or as many as 88 at the 8 somite stage (8 ss) in a group of wild-type embryos (Fig. 1). Reported KV measurements are also highly variable in the literature. A recent meta-analysis of several published studies shed light on the significant differences among reported KV cilia lengths, cilia numbers and flow strengths (Vandenberg et al., 2013). Taking a similar approach, we sampled published KV data collected at multiple stages of development to assess variations in KV cilia and size. This analysis revealed large variabilities in KV ciliated cell number, cilia length and lumen area in wild-type embryos (Table 1) that served as controls for experimental treatments in most studies. The average number of cilia per wild-type KV ranged from 22 cilia (Rosenfeld et al., 2013) to 90 cilia (Shu et al., 2007). Beyond these extremes, average wild-type KV cilia numbers have been reported to be in the 30s, 40s, 50s, 60s or 70s (Table 1). The average length of KV cilia was also variable, ranging from 2.6 μm (Krock and Perkins, 2014) to 7.9 μm (May-Simera et al., 2010) at 8–10 ss, but this variability may reflect different methods of measuring 3-dimensional (3D) cilia in 2D images. The size of KV, which is not often analyzed, is typically represented by the area of the lumen at its maximum diameter, which we refer to as KV^{max} area. In wild-type embryos, KV^{max} area has been reported to average as low as 2250 μm^2 (Navis et al., 2013) and as high as 4517 μm^2 (Bonetti et al., 2014) at 10 ss (Table 1). This high degree of variability in KV measurements has makes it a challenge to compare results across studies and has complicated interpretations of what is to be considered as a significant defect that may impact LR patterning.

One potential source of KV variability is the developmental stage selected to perform the analysis. Previous reports have shown KV cilia elongate and KV organ size expands between 1 ss and 10 ss (Okabe et al., 2008; Oteiza et al., 2008; Wang et al., 2012). In contrast, the number of ciliated KV cells remained constant during these stages once the cilia elongate to a point that they can be easily identified (Okabe et al., 2008; Oteiza et al., 2008; Wang et al., 2011; Wang et al., 2012). We hypothesized that the amount of KV variability observed is stage-dependent. To test this, we characterized KV variation in wild-type populations over developmental time by characterizing fixed KVs at 4, 6, 8, and 10 ss. Antibodies that recognize aPKC were used to mark apical (luminal) surfaces of KV cells and acetylated Tubulin (Ac-Tub) antibodies labeled KV cilia (Fig. 1A–C). For each stage

analyzed, we pooled measurements of individuals from three independent clutches of embryos from the wild-type TAB strain collected on different days. In each embryo, the number of KV cilia (Fig. 1D), the length of these cilia (Fig. 1E) and the KV^{max} area of the lumen (Fig. 1F) were measured. The data are presented in box and whisker plots where the whiskers indicate the highest and lowest values to illustrate the range of measurements. To analyze the variation of these measurements, we calculated one standard deviation (sd) as a percentage of the mean (Fig. 1G). This revealed that KV cilia length had the smallest amount of variability (sd ranged between 6.7% to 9.6%) during development, whereas KV cilia number (sd range 25.3% to 42.3%) and KV lumen area (sd range 31.6% to 44.1%) showed large amounts of variability at each stage. Variation in KV cilia number and lumen area was lower at 8 ss and 10 ss than earlier stages, indicating some variability was indeed stage-specific. These results show that cilia length is relatively tightly controlled during development, whereas KV size—which is impacted by both the number of ciliated cells in the organ and the extent of lumen expansion—is highly variable. This analysis also indicates KVs are less variable in wild-type populations at later stages (8–10 ss), suggesting measurements at these stages provide a more accurate description of KV.

Analysis of several zebrafish strains reveals similar variabilities in KV formation

We also investigated whether specific features of KV (cilia number, cilia length or lumen size) developed differently in different zebrafish strains. We hypothesized modifiers in specific genetic backgrounds may impact KV development. To test this, we compared KVs at 8 ss in three different wild-type strains—TAB, AB, and TL—and several transgenic strains (Fig. 2A–C). Each of the wild-type strains had similar mean values for KV cilia length (Fig. 2E), but showed differences in KV cilia number (Fig. 2D) and KV^{max} area (Fig. 2F). Interestingly, KVs in AB embryos had, on average, fewer than 40 cilia and a KV^{max} area less than 2000 μm^2. Such variations in KV size among wild-type strains are reminiscent of the variabilities reported in the literature (Table 1) and suggest that differences in KV size are, at least in part, due to differences in wild-type strain backgrounds. We next analyzed transgenic strains obtained from different sources that are used to study KV development and LR patterning: 1) *Tg(sox17:GFP)*^{s870} (Sakaguchi et al., 2006); GFP is expressed in DFC/KV cells and endoderm, 2) *Tg(sox17:DsRed)*^{s903} (Chung and Stainier, 2008); RFP is expressed in DFC/KV cells and endoderm 3) *Tg(dusp6:GFP-MA)*^{pt19} (Wang et al., 2011); membrane-targeted GFP is expressed in FGF responsive cells that include the DFC/KV cell lineage, 4) *Tg(h2afx:EGFP-rab11a)*^{mw6} (Clark et al., 2011); a Rab11a-GFP fusion protein is ubiquitously expressed, 5) *Tg(myl7:GFP)*^{f1} (Huang et al., 2003); GFP is expressed in cardiomyocytes and 6) *TgBAC(cftr:GFP)*^{pd1041} (Navis et al., 2013); a Cftr-GFP fusion protein is expressed in KV. Each of these strains should have a mixed background; most were generated using the AB strain (see materials and methods) and have subsequently been maintained in our animal facility by outcrossing with TAB fish. We found that nearly all transgenic strains analyzed showed very similar mean values for KV cilia number, cilia length and KV^{max} area (Fig. 2D–F). One exception was the *Tg(h2afx:EGFP-rab11a)*^{mw6} transgenic strain (Fig. 2C), in which KVs consistently showed a reduced number of cilia, reduced cilia length, and lumen area (Fig. 2D–F). These findings are in line with the previous reports that link Rab11a function to KV development (Tay et al., 2013; Westlake et al., 2011), suggesting expression of the Rab11a fusion protein is responsible for altering KV

development. Analysis of variation using percent standard deviation revealed that each of the wild-type and transgenic strains, again with the exception of *Tg(h2afx:EGFP-rab11a)*^{mw6} which showed greater variance, showed similar amounts of variability in KV size, cilia length, and cilia number at 8 ss (Fig. 2G). These results indicated that the amount of variation in KV development is similar within the individual strains we selected, but modifiers in different genetic backgrounds might explain variability among KV studies that have used different wild-type strains.

KV size correlates with cilia number but is separable from cilia length

This study (Fig. 1) and others (Okabe et al., 2008; Oteiza et al., 2008; Wang et al., 2012) have recognized that KV cilia elongation proceeds in-step with lumen expansion, which suggests ciliogenesis may be mechanistically linked with lumenogenesis during development. However, recent studies (Navis et al., 2013; Tay et al., 2013) have challenged this idea by providing evidence that cilia formation is independent of lumen size. To investigate the relationship between KV lumen size and KV cilia development in a large cohort of embryos, we pooled data points obtained for KVs in the different transgenic strains we analyzed (n=292 embryos). A modest correlation (R^2 value of 0.436) was observed between KV lumen size and cilia number among the strains (Fig. 2H). This suggested that the number of ciliated cells incorporated into KV plays a role in KV development, but is not the only determinant of KV organ size. This finding is consistent with results that show fluid secretion regulated by the cystic fibrosis transmembrane conductance regulator (Cftr) protein is important for expanding KV lumen size (Navis et al., 2013). Zebrafish with *cftr* mutations developed LR patterning defects and showed a reduced or absent KV lumen. Interestingly, the number and length of KV cilia was similar in wild-type and mutant KVs. In our analysis of wild-type embryos, we found virtually no correlation (R^2 value of 0.052) between KV^{max} area and KV cilia length (Fig. 2I). This result supports observations that cilia length is not dependent on lumen size (Navis et al., 2013; Tay et al., 2013) and that regulators of ciliogenesis can be uncoupled from regulators of lumenogenesis in KV.

Modulation of Cftr alters KV size, but not necessarily LR patterning

The relationship between KV lumen size and KV function has remained unclear. We took advantage of modulating Cftr levels, which alters KV size without altering KV cilia (Fig. 3A–D), to specifically investigate the role of KV size in LR patterning. To increase KV size, we used the small molecule CFTact-09 that enhances Cftr function (Ma et al., 2002). Wild-type embryos treated with CFTact-09 between bud stage and 8 ss showed an average KV^{max} area of 4678 ± 1380 μm^2 that was ~50% larger than vehicle controls (3124 ± 855 μm^2) (Fig. 3I). In treated embryos, KV cilia numbers (Fig. 3J) and lengths (Fig. 3K) were similar to controls. Analysis of *spaw* expression by RNA in situ hybridization (Fig. 3E–H) indicated that the increased KV size did not alter LR patterning (Fig. 3L). To reduce KV size, we used previously characterized hypomorphic *cftr*^{pd1048} mutants (Navis et al., 2013) or a suboptimal dose of anti-sense morpholino oligonucleotides (MO) designed to interfere with Cftr translation. As previously described (Navis et al., 2013), *cftr*^{pd1048} homozygous mutants showed *spaw* asymmetry defects in ~50% of the population (Fig. 3L) and KVs in these embryos had significantly reduced lumen size, but unaffected cilia number and length (Fig. 3I–K). Measurements of KV^{max} area revealed a mean of 1343± 587 μm^2 in mutants as

compared to 3308± 670 μm^2 in wild-type siblings. By titrating the dose of Cftr MO, we found that injecting 1 ng of Cftr MO reduced the average KV^{max} area to 1755± 505 μm^2 that was significantly smaller than controls (3127± 1256 μm^2) but slightly larger than *cftr*^{pd1048} mutants (Fig 3I). Intriguingly, *spaw* asymmetry was predominantly normal in Cftr morphant embryos: 83% had left-sided *spaw* expression (Fig. 3L). Since KV cilia parameters were similar between *cftr*^{pd1048} mutants and Cftr morphants (Fig. 3J–K), it appeared the difference in penetrance of LR patterning defects might be due to the slight difference in KV size. Thus, these results suggested a KV size threshold exists between 1300μm^2 and 1700μm^2, below which KV can no longer function to generate robust LR asymmetric development of the embryo.

Identification of a KV size threshold necessary for LR patterning

To test the hypothesis that a KV size threshold must be exceeded for reliable KV function, we used the inherent variability in KV size (Fig. 1) to analyze the relationship between KV size and LR patterning in individual wild-type embryos. Wild-type (TAB) clutches were screened under a dissecting microscope to qualitatively identify embryos with a small, average sized or large KVs at either 8 ss, when cilia generate robust fluid flows in KV (Wang et al., 2012), or at the earlier 2–3 ss stage when intraciliary Ca^{2+} activity peaks (Yuan et al., 2015). For each embryo, KV was imaged using differential interference contrast (DIC) microscopy (at 8 ss or 3 ss) to determine KV^{max} area (Fig. 4A–D). Each embryo was then maintained individually and allowed to develop until 18 ss when the LR axis had been determined. To assess LR patterning, individual embryos were analyzed via single-embryo RNA in situ hybridization for *spaw* expression (Fig. 4A′–D′). This allowed for direct comparison of KV size to expression of the LR marker in each embryo. For embryos in which KV size was measured at 8 ss, plotting the *spaw* results for each embryo (n=84) as either normal (left-sided) or altered (right-sided, bilateral or absent) indicated that embryos with smaller KVs had a higher likelihood of developing LR defects (Fig. 4E). We next grouped these *spaw* results based on the embryos' KV^{max} area (Fig. 4F), which showed that embryos with a KV^{max} area greater than 1300 μm^2 had predominantly normal left-sided *spaw* expression (>70% of the population was normal) and the majority of the embryos with KVs below 1300 μm^2 showed altered *spaw* expression (<40% of the embryos were normal). When measured at 3 ss, KV size did not correlate with *spaw* asymmetry (Fig. 4G–H), which is consistent with observations that KV is rapidly expanding during this stage and has not yet reached its final size. Taken together, these results indicated that by the 8 ss stage KV must exceed a size threshold of approximately 1300 μm^2 for robust LR patterning of the embryo.

Discussion

A ciliated organ of asymmetry plays a key role in generating LR patterning information in vertebrate embryos. The zebrafish KV has been a workhorse for discovering genes that control organ of asymmetry development, but significant variations in KV size and cilia observed in different studies (see Table 1) have made it challenging to evaluate the relationship between KV form and function. For example, KVs with an average of 30 cilia in a LR patterning mutant may be significantly different from KVs in wild-type siblings that

had an average of 50 cilia in one study, whereas an average of 30 cilia was considered normal in another study. Here, we sought to better understand variations in KV development and determine the role of KV size in establishing LR asymmetry. We quantified variabilities in KV size and KV cilia at different stages in wild-type embryos and in several transgenic strains that are commonly used in LR studies. KV cilia length had the smallest amount of variability, whereas KV cilia number and lumen size showed large variabilites within similar stages and genetic backgrounds. In addition, we found a modest correlation between KV size and cilia number, but no correlation between KV size and cilia length. Lastly, we identified a KV size threshold that is necessary for proper KV function to break symmetry, which provides an explanation for wide-ranging variabilities observed in KV development.

Variations in KV development may reflect developmental noise

It is clear from this study (Fig. 1) and others (Table 1) that KV organ size is not tightly controlled. Instead, KV formation appears to be a process that is significantly influenced by developmental noise. Phenotypic variations that occur among individuals with a similar genotype and environment are often thought to result from noisy biochemical processes at the cellular level, such as stochastic gene expression or signal transduction (Raser and O'Shea, 2005). The underlying causes for noisy KV development are not clear. Since zebrafish strains are not isogenic, small genetic differences (e.g. polymorphisms) that modulate gene expression could account for some KV variation among individuals. Our analysis of several different zebrafish wild-type and transgenic strains indicated the variation in KV development was quite similar in different genetic backgrounds (Fig. 2), suggesting the amount of variability observed is not strain-specific. Another possibility is that noise in KV comes from stochastic signaling or gene expression that regulates KV development. Interestingly, the number of precursor DFCs that give rise to KV is variable from embryo to embryo. We recently quantified the number of DFCs at several stages of development (Gokey et al., 2015) and found that the number of DFCs ranged from 16 to 27 (average ±one sd = 20±3 DFCs) at 60% epiboly stage soon after DFCs are first specified. At bud stage, after the cells have proliferated and are about to differentiate into KV cells, the number of DFCs ranged from 33 to 72 (average = 50±8 DFCs). This suggests noisy signaling that mediates DFC specification and/or proliferation contributes to variations in KV organ size. DFC specification is regulated by Nodal (Tgfβ) signaling (Oteiza et al., 2008), making it possible that stochastic changes in Nodal signaling strength could influence the number of DFCs specified. We identified the vacuolar-type H^+-ATPase (V-ATPase) proton pump as the first known regulator of DFC proliferation during epiboly stages (Gokey et al., 2015). Interfering with V-ATPase activity reduced DFC proliferation, which resulted in small KVs. Random fluctuations of V-ATPase activity could alter DFC proliferation enough to vary the number of DFCs that differentiate and incorporate into the KV organ in a given embryo. Additional studies designed to track and manipulate the specification and proliferation of DFCs as they mature to form KV will be needed to further test the role of developmental noise during these stages of DFC/KV formation.

KV lumen size does not restrict cilia elongation

In contrast to noisy development of KV size, KV cilia length is tightly controlled (Fig. 1). Such tight control indicates there is an optimal cilia length for generating functional flows in

KV. Indeed, perturbations of the mTOR signaling pathway that impacts cilia elongation revealed that making cilia either too short or too long will disrupt KV fluid flows and LR patterning (Yuan et al., 2012). Observations that KV cilia elongate concomitantly with lumen expansion during development (Fig. 1; Okabe et al., 2008; Oteiza et al., 2008) suggested a potential link between these processes. One might predict that the lumen must expand properly to provide enough space for the cilia to grow and that feedback mechanisms exist that couple ciliogenesis to lumenogenesis. However, recent studies in *cftr* mutants have shown that KV cilia elongate to normal length even when the lumen does not expand (Navis et al., 2013). Similarly, experiments probing genetic interactions between the Lethal giant larvae 2 (Lgl2) cell polarity protein and the Rab11a small GTPase (Tay et al., 2013) resulted in normal cilia in KVs with reduced lumen size. Here, we tested the relationship of KV size and cilia for the first time in wild-type embryos (e.g. no genetic perturbations that may have unrecognized effects) and found no correlation between KV lumen size and cilia length (Fig. 2I). The distribution of average KV cilia lengths were similar regardless of the lumen area, indicating tight control of KV cilia length occurs independent of KV lumen formation. Our analysis of wild-type embryos support the findings from the genetic studies that indicate cilia elongation can be uncoupled from lumen expansion in the developing KV.

A KV size threshold for robust function

Our analysis of Cftr-modulated embryos (Fig. 3) and individual wild-type embryos (Fig. 4) suggests that KV development does not need to be tightly controlled, but rather must only exceed a size threshold (KV^{max} area of ~1300 μm^2 at 8 ss) to function robustly in LR patterning. A threshold mechanism explains why KV development can be so noisy: as long as KV grows beyond the threshold it can function sufficiently to generate normal LR signals >70% of the time. Thus, once past the threshold, it appears KV size does not have much impact on function. A size threshold also explains how the KV organ can function at the same time it is expanding in size. The KV lumen is continuously growing larger in wild-type embryos between 1 to 8 ss (Oteiza et al., 2008), which are stages that are critical for KV functions associated with LR patterning: at 1–4 ss KV cilia become motile and intraciliary Ca^{2+} fluxes peak (Yuan et al., 2015); at 4–6 ss KV remodeling packs more ciliated cells into the dorsoanterior region of KV, which corresponds with the onset of strong leftward flow across the anterior pole of KV (Wang et al., 2012); at 6–8 ss asymmetric Ca^{2+} signaling is detected in mesendoderm (Yuan et al., 2015); at 8–10 ss asymmetric expression of the Nodal/Spaw antagonist *charon* is detected near KV (Hashimoto et al., 2004); and finally at 10–12 ss left-sided *spaw* expression is initiated in lateral plate mesoderm (Long et al., 2003). In wild-type embryos the minimum KV^{max} area of ~1300 μm^2 is met by 4 ss (Fig. 1F); thus at subsequent stages the size of the organ (even if it over-expands) would not impact function. Consistent with this idea, our analysis of exceptionally large KVs indicates that increased size does not interfere with KV function. In fact, 100% of large KVs (KV^{max} area >3300 μm^2) in embryos treated with CFTact-09 (Fig. 3; n=28) or in the wild-type population (Fig. 4; n=24) were associated with normal *spaw* asymmetry.

A size threshold indicates that KV lumen formation plays a critical role in establishing LR asymmetry. However, what is the role of KV size? Our results suggest that KV size is not critical at early stages (3 ss) during intraciliary Ca^{2+} fluxes, but rather plays an important

role at later stages (8 ss) when cilia generate strong asymmetric flows (Fig. 4). The size of the KV lumen likely has a significant impact on flow dynamics that are essential for LR development (Sampaio et al., 2014). Previous work found disorganized flows in *cftr*^{pd1048} mutant KVs (Navis et al., 2013) that we found to have an average KV^{max} area of 1343±587 μm^2. Similar to these results, we predict flows to be altered in wild-type embryos with KV sizes that fall below 1300 μm^2. Another study found that lumen expansion is necessary for KV remodeling that concentrates ciliated cells in the dorsoanterior region of KV (Compagnon et al., 2014) to drive strong leftward flows. It is likely that tensions created by the expanding fluid-filled lumen play a key role in regional cell shape changes during KV remodeling. To begin to characterize flow dynamics in small KVs in wild-type embryos, we imaged naturally occurring debris in KV as described (Sampaio et al., 2014). We observed normal flow of particles in KVs with a KV^{max} area >1700 μm^2, but, intriguingly, we did not find particles to track in KVs ≤1300 μm^2 (n=3 embryos). Developing new tracking approaches may be useful for visualizing and measuring flows in small KVs. Another possible role for size is to ensure a sufficient number of cilia are present in KV to generate asymmetric fluid flow. Modeling simulations have suggested approximately 30 functional cilia are necessary to break LR symmetry (Sampaio et al., 2014). Interestingly, this number of cilia appears to be quite consistent with the threshold of KV size described here. We found that a KV^{max} area threshold of 1300 μm^2 falls approximately 1.5 sd from the mean area (3127 μm^2) at 8ss. Similarly, 1.5 sd from the mean of 52 cilia in wild-type embryos is 28 cilia, which is very close to the predicted 30 cilia needed for LR patterning. Thus, embryos with KVs below the threshold are likely to develop LR patterning defects due to insufficient flows caused by insufficient and/or mis-positioned cilia.

In summary, we have characterized developmental variation during KV formation and found a minimum KV organ size that is required for its function to direct asymmetric left-sided *spaw* expression. Intriguingly, unexplained defects in LR asymmetric *spaw* expression are commonly observed in ~5–10% of wild-type populations of zebrafish embryos (see controls in Fig. 3L for examples). These defects could be due to variations in KV formation. During our analysis of individual wild-type embryos, we found that < 0.5% of KVs fall below the size threshold, suggesting failure to exceed the threshold does not fully account for altered *spaw* expression in wild type populations. It is likely that some of these *spaw* LR defects are due to variations in other aspects of KV development that are vital for function, including cilia length (Lopes et al., 2010; Neugebauer et al., 2009), cilia motility (Gao et al., 2010; Sampaio et al., 2014) and KV cell shapes that control cilia positioning (Compagnon et al., 2014; Wang et al., 2012). Additional studies will be necessary to further understand how regulation of each of these processes is integrated within the context of noisy KV size development. The identification of a KV size threshold for robust function provides new insight into the role of organ of asymmetry size during LR patterning and offers an explanation for how the zebrafish embryo can tolerate large variations in KV developmental outcomes.

Material and Methods

Zebrafish

Embryos collected from natural matings were staged as described (Kimmel et al., 1995). Wild-type strains TL (tupfle long fin) and AB were obtained from the Lewis lab (Syracuse University). Wild-type TAB and the transgenic strains *Tg(sox17:GFP)*^{s870} (generated on the wild-type AB background) and *Tg(sox17:DsRed)*^{s903} (AB background) were obtained from the Zebrafish International Resource Center (ZIRC). *Tg(dusp6:GFP-MA)*^{pt19} fish (AB background) were obtained from the Tsang Lab (University of Pittsburg), *Tg(h2afx:EGFP-rab11a)*^{mw6} fish (AB background) were provided by the Link Lab (Medical College of Wisconsin), *Tg(myl7:GFP)*^{f1} fish (unknown background) were obtained from the Yost Lab (University of Utah) and *TgBAC(cftr:GFP)*^{pd1041} and *cftr*^{pd1048} fish (AB background) were provided by the Bagnat Lab (Duke University). It is important to note that all transgenic and mutant strains have been maintained in the Amack lab via outcrosses with wild-type TAB fish.

Microinjections

All embryo microinjections were performed between the 1- to 4-cell stages. Morpholinos (MO) were obtained from Gene Tools, LLC. A standard negative control MO (5′-CCTCTTACCTCAGTTACAATTTATA-3′) was injected at a 3 ng dose and Cftr MO (5′-CACAGGTGATCTCTGCATCCTAAA-3′) was injected at a 1 ng dose.

Pharmacological treatments

Embryos were treated with either 10 μM CFTact-09 (Chem Bridge) (Ma et al., 2002) in 1% DMSO or a vehicle control of 1% DMSO alone from the bud stage to 8 ss. At 8 ss the drug or DMSO were removed and the embryos were washed with embryo media. Embryos were either fixed at 8 ss for fluorescent immunostaining of KV or grown to 18 ss for *spaw* analysis.

RNA in situ hybridizations and fluorescent immunostaining

Whole-embryo RNA in situ hybridization analysis of *spaw* was performed as previously described (Wang et al., 2011). For immunostaining, embryos were fixed overnight at 4° C in 4% paraformaldehyde in PBS with 0.5% Triton X-100 and then processed for whole mount antibody staining as described (Tay et al., 2013). Primary antibodies were: anti-aPKC (Santa Cruz sc-216) (1:200 dilution) and anti-acetylated tubulin (Sigma T6793) (1:400). AlexaFluor 488 and 568 (anti mouse and anti-rabbit) fluorescent secondary antibodies (Invitrogen) were used at 1:200 dilutions. Embryos were imaged using a Zeiss AxioImager M1 compound microscope or a Perkin-Elmer Ultra View Vox spinning disk confocal microscope. When necessary, images were rotated for uniform orientations with anterior at top.

Quantitative analysis of Kupffer's vesicle size and cilia

KV metrics were quantified in embryos immunostained with aPKC and acetylated-tubulin antibodies at stated developmental stages. KV cilia number, cilia length and KV^{max} area of

the lumen were measured using ImageJ software (NIH). KV^{max} area was defined by manually outlining aPKC staining at the largest diameter. For single-embryo analysis to directly correlate KV size with *spaw* expression, DIC microscopy was used to image KVs in live embryos mounted in low melting agarose at 8 ss. The widest KV diameter was used to calculate KV^{max} area of the lumen. Embryos were removed from the agarose and cultured individually until 18 ss, when they were fixed for *spaw* analysis via single-embryo RNA in situ hybridization.

Statistical analyses

Variances were determined using one standard deviation (sd) of the mean and correlations were analyzed using the Coefficient of Determination (R^2). Both sd and R^2 values were calculated using Excel software (Microsoft). For analyses between two groups of embryos, differences were considered statistically significant when $p<0.05$ as determined using Student's T-Test.

Acknowledgments

We thank Shramika Adhikary and Sharleen Buel for technical assistance and the Lewis, Tsang, Link, Yost and Bagnat labs for providing zebrafish strains. This work was funded by the National Institute of Health National Heart, Lung, and Blood Institute (NHLBI) grant R01HL095690 to J.D.A.

References

Afzelius BA. A human syndrome caused by immotile cilia. Science. 1976; 193:317–319. [PubMed: 1084576]

Amack JD. Salient features of the ciliated organ of asymmetry. Bioarchitecture. 2014; 4:6–15. [PubMed: 24481178]

Bisgrove BW, Makova S, Yost HJ, Brueckner M. RFX2 is essential in the ciliated organ of asymmetry and an RFX2 transgene identifies a population of ciliated cells sufficient for fluid flow. Dev Biol. 2012; 363:166–178. [PubMed: 22233545]

Blum M, Weber T, Beyer T, Vick P. Evolution of leftward flow. Seminars in cell & developmental biology. 2009; 20:464–471. [PubMed: 19056505]

Bonetti M, Paardekooper Overman J, Tessadori F, Noel E, Bakkers J, den Hertog J. Noonan and LEOPARD syndrome Shp2 variants induce heart displacement defects in zebrafish. Development. 2014; 141:1961–1970. [PubMed: 24718990]

Caron A, Xu X, Lin X. Wnt/beta-catenin signaling directly regulates Foxj1 expression and ciliogenesis in zebrafish Kupffer's vesicle. Development. 2012; 139:514–524. [PubMed: 22190638]

Cartwright JH, Piro O, Tuval I. Fluid-dynamical basis of the embryonic development of left-right asymmetry in vertebrates. Proc Natl Acad Sci U S A. 2004; 101:7234–7239. [PubMed: 15118088]

Chen Y, Wu B, Xu L, Li H, Xia J, Yin W, Li Z, Shi D, Li S, Lin S, Shu X, Pei D. A SNX10/V-ATPase pathway regulates ciliogenesis in vitro and in vivo. Cell Res. 2012; 22:333–345. [PubMed: 21844891]

Chung WS, Stainier DY. Intra-endodermal interactions are required for pancreatic beta cell induction. Dev Cell. 2008; 14:582–593. [PubMed: 18410733]

Clark BS, Winter M, Cohen AR, Link BA. Generation of Rab-based transgenic lines for in vivo studies of endosome biology in zebrafish. Dev Dyn. 2011; 240:2452–2465. [PubMed: 21976318]

Compagnon J, Barone V, Rajshekar S, Kottmeier R, Pranjic-Ferscha K, Behrndt M, Heisenberg CP. The notochord breaks bilateral symmetry by controlling cell shapes in the zebrafish laterality organ. Dev Cell. 2014; 31:774–783. [PubMed: 25535919]

Cooper MS, D'Amico LA. A cluster of noninvoluting endocytic cells at the margin of the zebrafish blastoderm marks the site of embryonic shield formation. Dev Biol. 1996; 180:184–198. [PubMed: 8948584]

Essner JJ, Amack JD, Nyholm MK, Harris EB, Yost HJ. Kupffer's vesicle is a ciliated organ of asymmetry in the zebrafish embryo that initiates left-right development of the brain, heart and gut. Development. 2005; 132:1247–1260. [PubMed: 15716348]

Gao C, Wang G, Amack JD, Mitchell DR. Oda16/Wdr69 is essential for axonemal dynein assembly and ciliary motility during zebrafish embryogenesis. Dev Dyn. 2010; 239:2190–2197. [PubMed: 20568242]

Gokey JJ, Dasgupta A, Amack JD. The V-ATPase accessory protein Atp6ap1b mediates dorsal forerunner cell proliferation and left-right asymmetry in zebrafish. Dev Biol. 2015:DBIO1531.

Hashimoto H, Rebagliati M, Ahmad N, Muraoka O, Kurokawa T, Hibi M, Suzuki T. The Cerberus/Dan-family protein Charon is a negative regulator of Nodal signaling during left-right patterning in zebrafish. Development. 2004; 131:1741–1753. [PubMed: 15084459]

Hojo M, Takashima S, Kobayashi D, Sumeragi A, Shimada A, Tsukahara T, Yokoi H, Narita T, Jindo T, Kage T, Kitagawa T, Kimura T, Sekimizu K, Miyake A, Setiamarga D, Murakami R, Tsuda S, Ooki S, Kakihara K, Naruse K, Takeda H. Right-elevated expression of charon is regulated by fluid flow in medaka Kupffer's vesicle. Development, growth & differentiation. 2007; 49:395–405.

Hong SK, Dawid IB. FGF-dependent left-right asymmetry patterning in zebrafish is mediated by Ier2 and Fibp1. Proc Natl Acad Sci U S A. 2009; 106:2230–2235. [PubMed: 19164561]

Huang CJ, Tu CT, Hsiao CD, Hsieh FJ, Tsai HJ. Germ-line transmission of a myocardium-specific GFP transgene reveals critical regulatory elements in the cardiac myosin light chain 2 promoter of zebrafish. Dev Dyn. 2003; 228:30–40. [PubMed: 12950077]

Kimmel CB, Ballard WW, Kimmel SR, Ullmann B, Schilling TF. Stages of embryonic development of the zebrafish. Dev Dyn. 1995; 203:253–310. [PubMed: 8589427]

Kramer-Zucker AG, Olale F, Haycraft CJ, Yoder BK, Schier AF, Drummond IA. Cilia-driven fluid flow in the zebrafish pronephros, brain and Kupffer's vesicle is required for normal organogenesis. Development. 2005; 132:1907–1921. [PubMed: 15790966]

Krock BL, Perkins BD. The Par-PrkC polarity complex is required for cilia growth in zebrafish photoreceptors. PLoS One. 2014; 9:e104661. [PubMed: 25144710]

Lee JD, Anderson KV. Morphogenesis of the node and notochord: the cellular basis for the establishment and maintenance of left-right asymmetry in the mouse. Dev Dyn. 2008; 237:3464–3476. [PubMed: 18629866]

Lin X, Xu X. Distinct functions of Wnt/beta-catenin signaling in KV development and cardiac asymmetry. Development. 2009; 136:207–217. [PubMed: 19103803]

Liu DW, Hsu CH, Tsai SM, Hsiao CD, Wang WP. A variant of fibroblast growth factor receptor 2 (Fgfr2) regulates left-right asymmetry in zebrafish. PLoS One. 2011; 6:e21793. [PubMed: 21747958]

Long S, Ahmad N, Rebagliati M. The zebrafish nodal-related gene southpaw is required for visceral and diencephalic left-right asymmetry. Development. 2003; 130:2303–2316. [PubMed: 12702646]

Lopes SS, Lourenco R, Pacheco L, Moreno N, Kreiling J, Saude L. Notch signalling regulates left-right asymmetry through ciliary length control. Development. 2010; 137:3625–3632. [PubMed: 20876649]

Ma T, Vetrivel L, Yang H, Pedemonte N, Zegarra-Moran O, Galietta LJ, Verkman AS. High-affinity activators of cystic fibrosis transmembrane conductance regulator (CFTR) chloride conductance identified by high-throughput screening. J Biol Chem. 2002; 277:37235–37241. [PubMed: 12161441]

May-Simera HL, Kai M, Hernandez V, Osborn DP, Tada M, Beales PL. Bbs8, together with the planar cell polarity protein Vangl2, is required to establish left-right asymmetry in zebrafish. Dev Biol. 2010; 345:215–225. [PubMed: 20643117]

Metcalf D. The Autonomous Behaviour of Normal Thymus Grafts. The Australian journal of experimental biology and medical science. 1963; 41(SUPPL):437–447.

Metcalf D. Restricted Growth Capacity of Multiple Spleen Grafts. Transplantation. 1964; 2:387–392. [PubMed: 14144351]

Nakamura T, Hamada H. Left-right patterning: conserved and divergent mechanisms. Development. 2012; 139:3257–3262. [PubMed: 22912409]

Navis A, Marjoram L, Bagnat M. Cftr controls lumen expansion and function of Kupffer's vesicle in zebrafish. Development. 2013; 140:1703–1712. [PubMed: 23487313]

Neugebauer JM, Amack JD, Peterson AG, Bisgrove BW, Yost HJ. FGF signalling during embryo development regulates cilia length in diverse epithelia. Nature. 2009; 458:651–654. [PubMed: 19242413]

Neugebauer JM, Cadwallader AB, Amack JD, Bisgrove BW, Yost HJ. Differential roles for 3-OSTs in the regulation of cilia length and motility. Development. 2013; 140:3892–3902. [PubMed: 23946439]

Nonaka S, Shiratori H, Saijoh Y, Hamada H. Determination of left-right patterning of the mouse embryo by artificial nodal flow. Nature. 2002; 418:96–99. [PubMed: 12097914]

Nonaka S, Tanaka Y, Okada Y, Takeda S, Harada A, Kanai Y, Kido M, Hirokawa N. Randomization of left-right asymmetry due to loss of nodal cilia generating leftward flow of extraembryonic fluid in mice lacking KIF3B motor protein. Cell. 1998; 95:829–837. [PubMed: 9865700]

Okabe N, Xu B, Burdine RD. Fluid dynamics in zebrafish Kupffer's vesicle. Dev Dyn. 2008; 237:3602–3612. [PubMed: 18924242]

Oteiza P, Koppen M, Concha ML, Heisenberg CP. Origin and shaping of the laterality organ in zebrafish. Development. 2008; 135:2807–2813. [PubMed: 18635607]

Qian M, Yao S, Jing L, He J, Xiao C, Zhang T, Meng W, Zhu H, Xu H, Mo X. ENC1-like integrates the retinoic acid/FGF signaling pathways to modulate ciliogenesis of Kupffer's Vesicle during zebrafish embryonic development. Dev Biol. 2013; 374:85–95. [PubMed: 23201577]

Ramsdell AF. Left-right asymmetry and congenital cardiac defects: getting to the heart of the matter in vertebrate left-right axis determination. Dev Biol. 2005; 288:1–20. [PubMed: 16289136]

Raser JM, O'Shea EK. Noise in gene expression: origins, consequences, and control. Science. 2005; 309:2010–2013. [PubMed: 16179466]

Rosenfeld GE, Mercer EJ, Mason CE, Evans T. Small heat shock proteins Hspb7 and Hspb12 regulate early steps of cardiac morphogenesis. Dev Biol. 2013; 381:389–400. [PubMed: 23850773]

Sakaguchi T, Kikuchi Y, Kuroiwa A, Takeda H, Stainier DY. The yolk syncytial layer regulates myocardial migration by influencing extracellular matrix assembly in zebrafish. Development. 2006; 133:4063–4072. [PubMed: 17008449]

Sampaio P, Ferreira RR, Guerrero A, Pintado P, Tavares B, Amaro J, Smith AA, Montenegro-Johnson T, Smith DJ, Lopes SS. Left-right organizer flow dynamics: how much cilia activity reliably yields laterality? Dev Cell. 2014; 29:716–728. [PubMed: 24930722]

Schweickert A, Weber T, Beyer T, Vick P, Bogusch S, Feistel K, Blum M. Cilia-driven leftward flow determines laterality in Xenopus. Curr Biol. 2007; 17:60–66. [PubMed: 17208188]

Shinohara K, Kawasumi A, Takamatsu A, Yoshiba S, Botilde Y, Motoyama N, Reith W, Durand B, Shiratori H, Hamada H. Two rotating cilia in the node cavity are sufficient to break left-right symmetry in the mouse embryo. Nat Commun. 2012; 3:622. [PubMed: 22233632]

Shu X, Huang J, Dong Y, Choi J, Langenbacher A, Chen JN. Na,K-ATPase alpha2 and Ncx4a regulate zebrafish left-right patterning. Development. 2007; 134:1921–1930. [PubMed: 17442698]

Smith AA, Johnson TD, Smith DJ, Blake JR. Symmetry Breaking Cilia-Driven Flow in the Zebrafish Embryo. J Fluid Mech. 2012; 705:26–45.

Sutherland MJ, Ware SM. Disorders of left-right asymmetry: heterotaxy and situs inversus. American journal of medical genetics. Part C, Seminars in medical genetics. 2009; 151C:307–317.

Tay HG, Schulze SK, Compagnon J, Foley FC, Heisenberg CP, Yost HJ, Abdelilah-Seyfried S, Amack JD. Lethal giant larvae 2 regulates development of the ciliated organ Kupffer's vesicle. Development. 2013; 140:1550–1559. [PubMed: 23482490]

Tumaneng K, Russell RC, Guan KL. Organ size control by Hippo and TOR pathways. Curr Biol. 2012; 22:R368–379. [PubMed: 22575479]

Vandenberg LN, Lemire JM, Levin M. Serotonin has early, cilia-independent roles in Xenopus left-right patterning. Disease models & mechanisms. 2013; 6:261–268. [PubMed: 22899856]

Wang G, Cadwallader AB, Jang DS, Tsang M, Yost HJ, Amack JD. The Rho kinase Rock2b establishes anteroposterior asymmetry of the ciliated Kupffer's vesicle in zebrafish. Development. 2011; 138:45–54. [PubMed: 21098560]

Wang G, Manning ML, Amack JD. Regional cell shape changes control form and function of Kupffer's vesicle in the zebrafish embryo. Dev Biol. 2012; 370:52–62. [PubMed: 22841644]

Westlake CJ, Baye LM, Nachury MV, Wright KJ, Ervin KE, Phu L, Chalouni C, Beck JS, Kirkpatrick DS, Slusarski DC, Sheffield VC, Scheller RH, Jackson PK. Primary cilia membrane assembly is initiated by Rab11 and transport protein particle II (TRAPPII) complex-dependent trafficking of Rabin8 to the centrosome. Proc Natl Acad Sci U S A. 2011; 108:2759–2764. [PubMed: 21273506]

Yuan S, Li J, Diener DR, Choma MA, Rosenbaum JL, Sun Z. Target-of-rapamycin complex 1 (Torc1) signaling modulates cilia size and function through protein synthesis regulation. Proc Natl Acad Sci U S A. 2012; 109:2021–2026. [PubMed: 22308353]

Yuan S, Zhao L, Brueckner M, Sun Z. Intraciliary calcium oscillations initiate vertebrate left-right asymmetry. Curr Biol. 2015; 25:556–567. [PubMed: 25660539]

Zhai G, Gu Q, He J, Lou Q, Chen X, Jin X, Bi E, Yin Z. Sept6 is required for ciliogenesis in Kupffer's vesicle, the pronephros, and the neural tube during early embryonic development. Molecular and cellular biology. 2014; 34:1310–1321. [PubMed: 24469395]

Zhang M, Zhang J, Lin SC, Meng A. beta-Catenin 1 and beta-catenin 2 play similar and distinct roles in left-right asymmetric development of zebrafish embryos. Development. 2012; 139:2009–2019. [PubMed: 22535411]

Hightlights

- Kupffer's vesicle (KV) development is variable in wild-type populations.
- The amount of KV variability is similar among different genetic backgrounds.
- Cilia elongation is independent of KV lumen size.
- KV must exceed a size threshold to direct robust LR patterning of the zebrafish embryo.

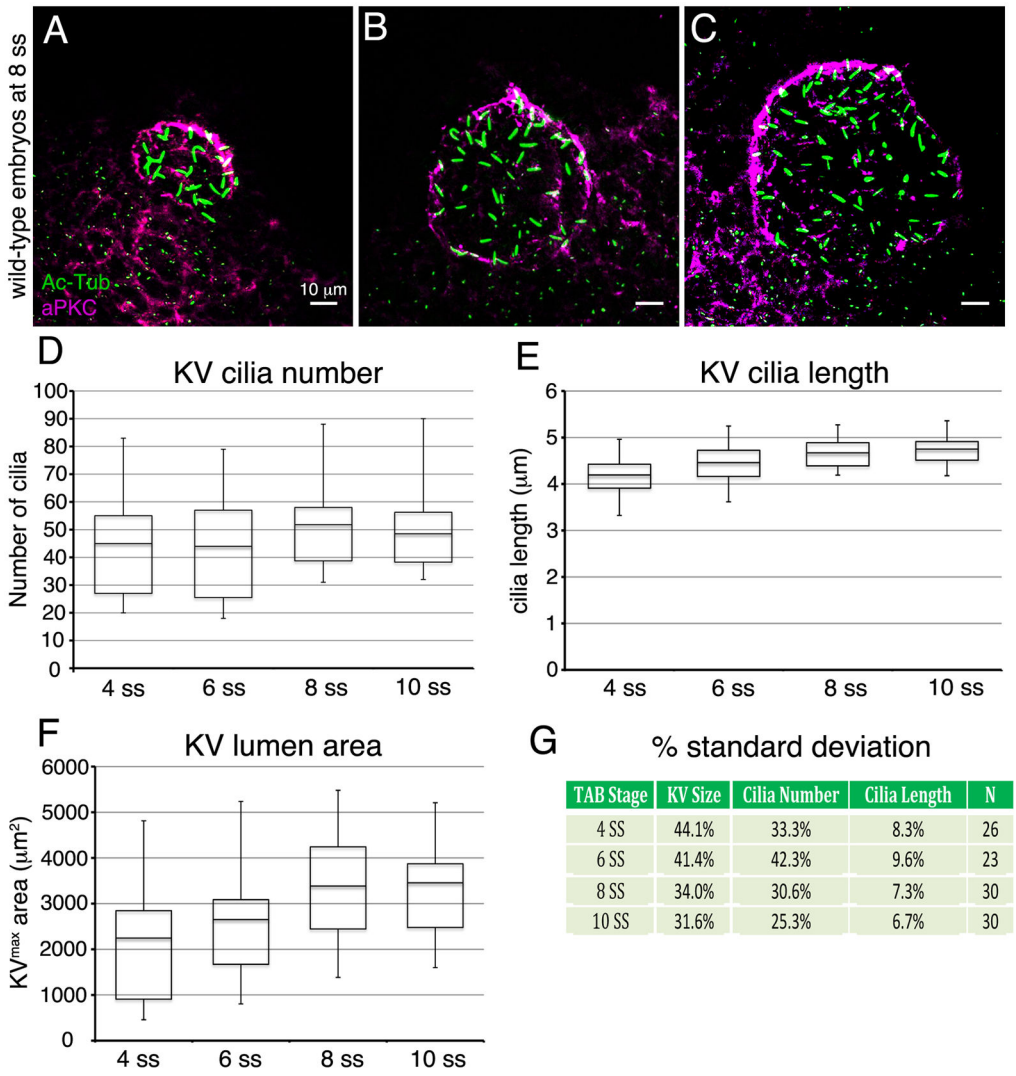

TAB Stage	KV Size	Cilia Number	Cilia Length	N
4 SS	44.1%	33.3%	8.3%	26
6 SS	41.4%	42.3%	9.6%	23
8 SS	34.0%	30.6%	7.3%	30
10 SS	31.6%	25.3%	6.7%	30

Figure 1. Analysis of variation in development of Kupffer's vesicle in wild-type embryos

(A–C) Representative maximum projections of confocal images of KV cells labeled with aPKC antibodies (magenta) to mark the KV lumen and acetylated Tubulin antibodies (green) to visualize cilia at 8 ss. These examples show a wild-type embryo with small KV size and few cilia (A) and embryos with an intermediate (B) or larger (C) lumen size. (D–F) Quantification of KV cilia number (D), cilia length (E) and lumen area (F) at 4 ss (n=26 embryos), 6 ss (n=23), 8 ss (n=30) and 10 ss (n=30). The horizontal line in the box and whisker plots indicates the mean and the whiskers show the minimum and maximum values. (G) Variations in cilia number, cilia length, and lumen size at each developmental stage are represented as one standard deviation converted to a percentage of the mean.

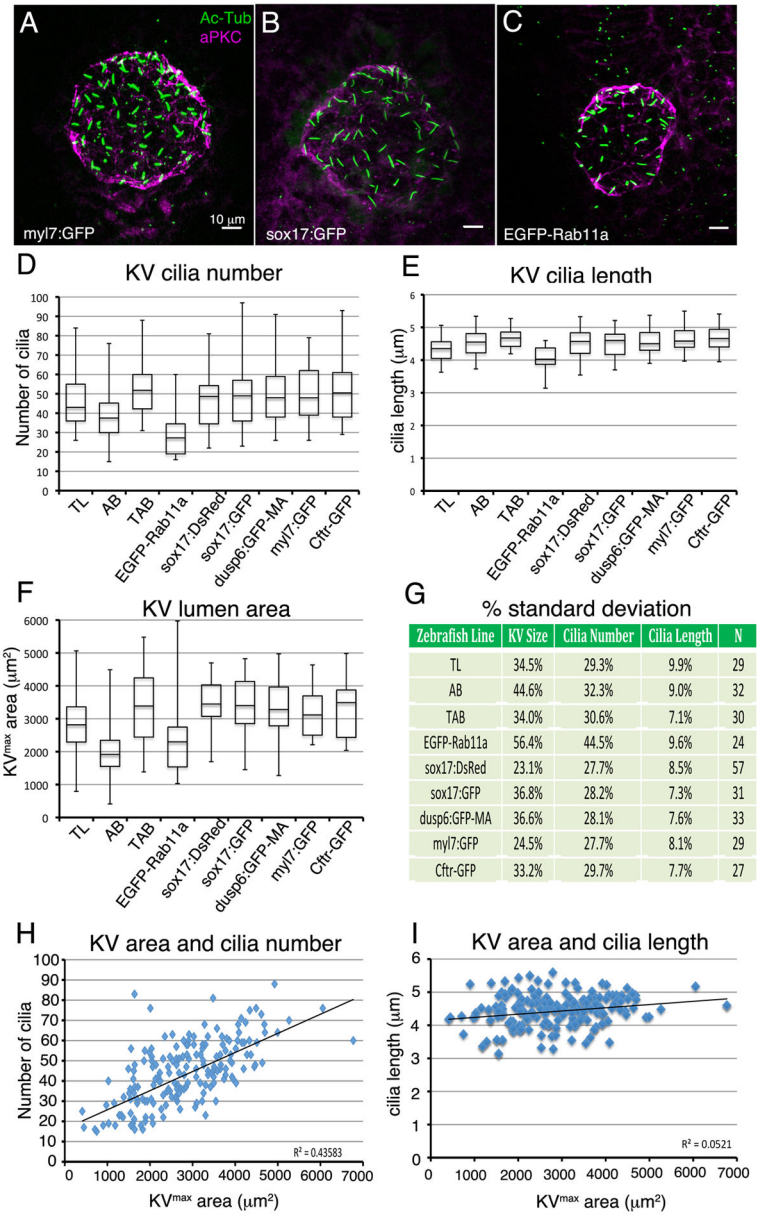

Zebrafish Line	KV Size	Cilia Number	Cilia Length	N
TL	34.5%	29.3%	9.9%	29
AB	44.6%	32.3%	9.0%	32
TAB	34.0%	30.6%	7.1%	30
EGFP-Rab11a	56.4%	44.5%	9.6%	24
sox17:DsRed	23.1%	27.7%	8.5%	57
sox17:GFP	36.8%	28.2%	7.3%	31
dusp6:GFP-MA	36.6%	28.1%	7.6%	33
myl7:GFP	24.5%	27.7%	8.1%	29
Cftr-GFP	33.2%	29.7%	7.7%	27

Figure 2. The amount of variation in Kupffer's vesicle development is similar among different wild-type and transgenic strains

(A–C) Images of KV at 8 ss from three different transgenic strains. KVs appeared similar in most strains, including *Tg(myl7:GFP)* (A) and *Tg(sox17:GFP)* (B), but were smaller in *Tg(h2afx:EGFP-rab11a)* (C). See text for descriptions of each strain. (D–F) Analysis of KV cilia number (D), cilia length (E) and lumen area (F) at 8 ss for different wild-type (TL and AB) and several transgenic strains. Data from wild-type TAB strain at 8 ss presented in Figure 1 is included for comparison. The number of embryos (N) analyzed for each strain is indicated in (G). (G) Variations in cilia number, cilia length, and lumen size are represented as one standard deviation as a percentage of the mean. (H–I) Analysis of potential correlations between KV lumen area and cilia number (H) and KV lumen area and cilia

length (I). Each point represents a single embryo (n=292 embryos). The R^2 (coefficient of determination) value is listed for all strains pooled.

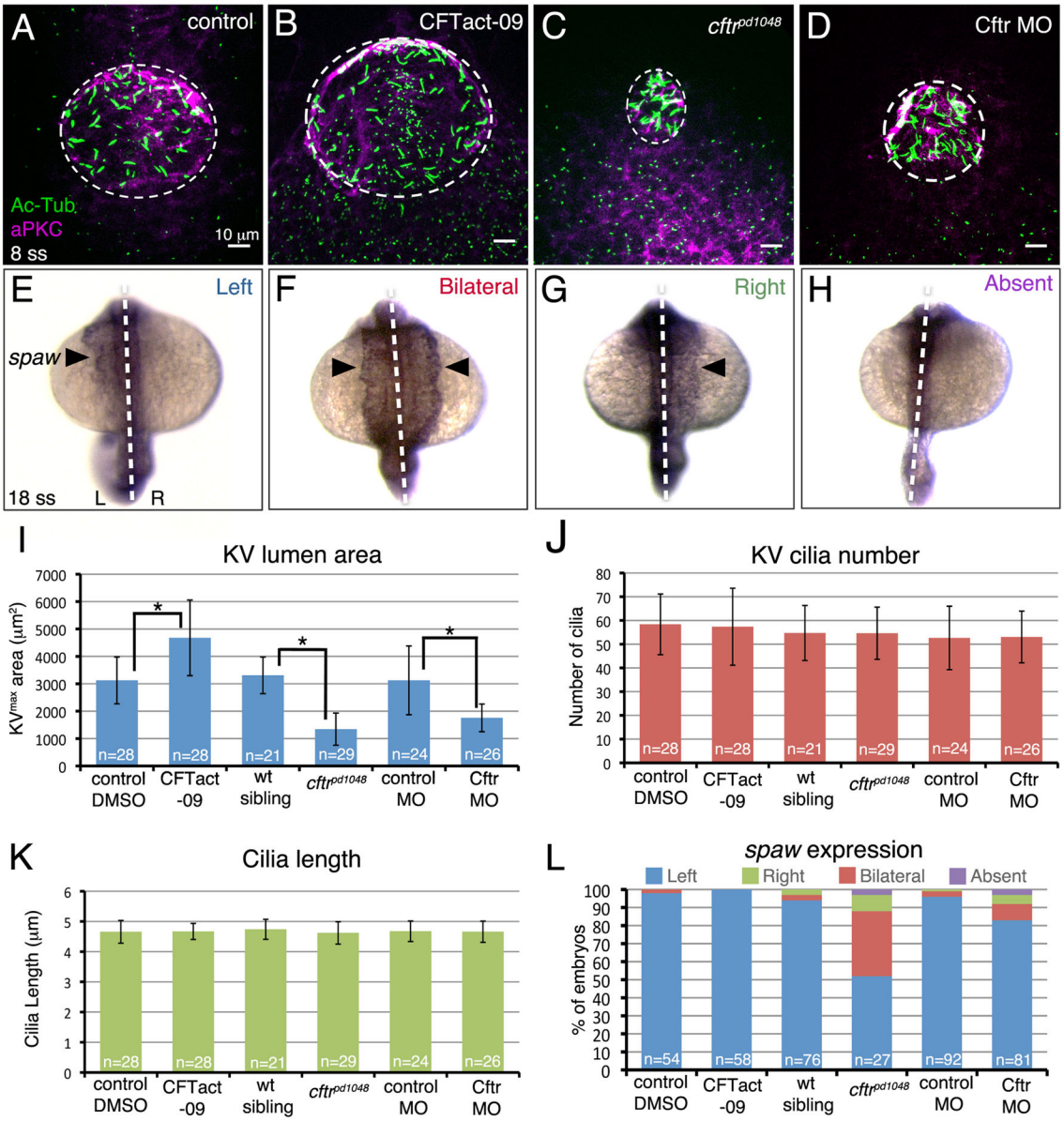

Figure 3. Role of Kupffer's vesicle size in LR patterning

(A–D) Modulating Cftr activity was used to alter KV lumen size at 8 ss. The Cftr activating drug CFTact-09 increased KV size (B), whereas a loss-of-function mutation (C) or morpholino (MO) interference (D) reduced KV size relative to controls (A). Dashed circles represent approximate KV lumen boundaries. (E–H) Possible outcomes of RNA in situ hybridization analysis of the LR patterning marker *spaw* in lateral plate mesoderm (arrowhead) at 18 ss are normal left-sided (E), bilateral (F), reversed right-sided (G) or absent (H) expression. Dashed lines indicate the embryonic midline. L=left; R=right. (I–K) Quantification of KV area (I), cilia number (J) and cilia length (K) in embryos with altered Cftr function and controls. (L) Analysis of *spaw* expression in Cftr modulated embryos. Error bars represent one standard deviation. n=number of embryos analyzed. * indicates $p < 0.05$

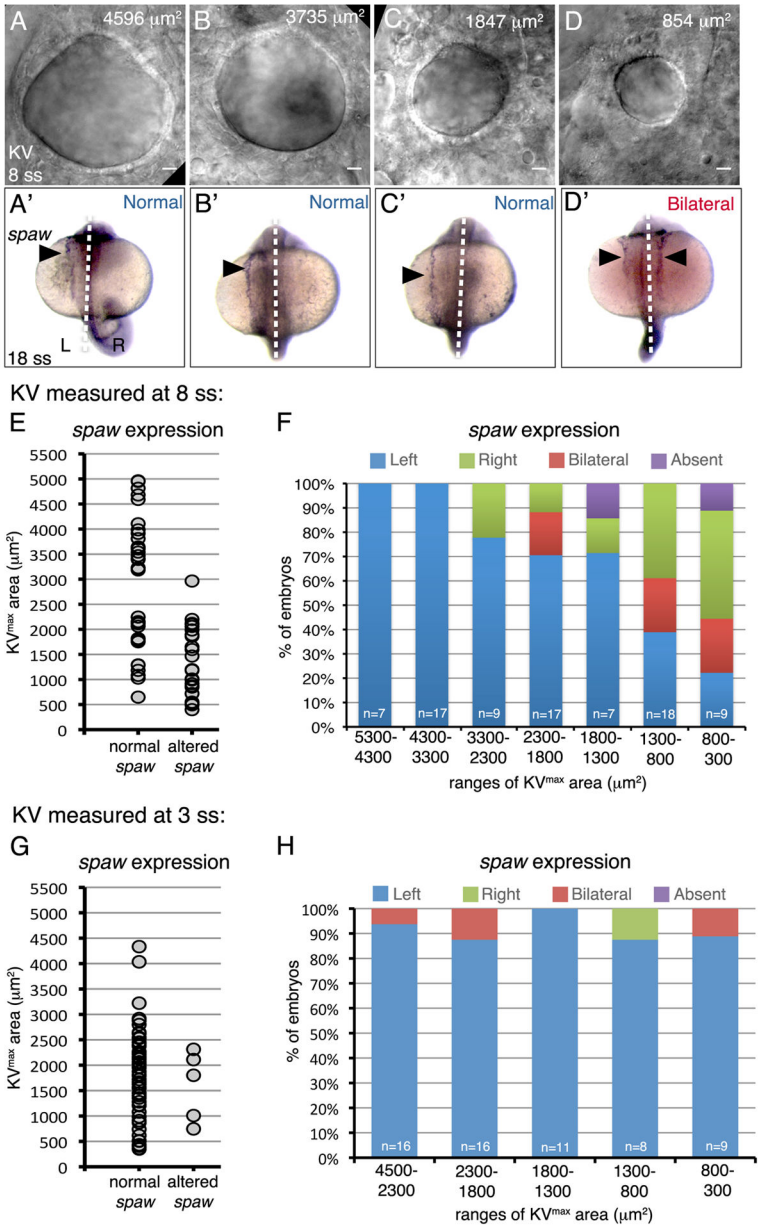

Figure 4. Identification of a Kupffer's vesicle size threshold necessary for robust LR patterning

(A–D) Representative DIC images of different sized KVs in living wild-type embryos at 8 ss. The KV^{max} area is indicated for each representative embryo. (A′–D′) *spaw* expression (arrowhead) at 18 ss in the same embryos. Dashed lines indicate the embryonic midline. L=left; R=right. (E–H) Analysis of *spaw* asymmetry in embryos in which KV was measured at 8ss (E–F) or 3 ss (G–H). (E, G) Normal (left-sided) and altered (bilateral, reversed or absent) *spaw* outcomes were plotted based on KV^{max} area. Each point represents a single embryo. (F, H) Observed *spaw* expression in embryos within specific ranges of KV^{max} areas. n=number of embryos analyzed.

Table 1

Selected published measurements that represent the variabilities in KV observed in wild-type embryos at multiple stages of development.

Developmental Stage	Average Number of Cilia per KV*	Average Length of KV Cilia (μm)*	Average KV Area (μm^2)*	Study Reference
1ss	62	1.2	nd	Oteiza, et al. 2008
2 ss	70	1.4	nd	Oteiza, et al. 2008
1–2 ss	29.6	2.6	nd	Okabe, et al. 2008
3 ss	45	5	nd	Qian, et al. 2013
4 ss	54.5	nd	nd	Neugebauer, et al. 2013
4 ss	70	3	nd	Oteiza, et al. 2008
3–4 ss	40.5	3.5	nd	Okabe, et al. 2008
5 ss	90	nd	nd	Hong and Dawid, 2009
5–6 ss	58.9	4.3	nd	Okabe, et al. 2008
6–8 ss	40	3.5	nd	Gao, et al 2011
7–8 ss	50.7	5.2	nd	Okabe, et al. 2008
8 ss	40.1	4.33	nd	Zhai, et al. 2014
8 ss	51.1	7	nd	Neugebauer, et al. 2013
8 ss	41	4	3300	Tay, et al. 2013
8 ss	37	4.5	3090	Wang, et al. 2011
8 ss	58	7.9	nd	May-Simera, et al. 2010
8–9 ss	42.2	5.97	nd	Bisgrove, et al. 2013
8–10 ss	31	2.6	nd	Krock and Perkins, 2014
8–10 ss	22	3.9	nd	Rosenfeld, et al. 2013
9–10 ss	49.0	6.4	nd	Okabe, et al. 2008
10 ss	51.4	4.2	4517	Bonetti, et al. 2014
10 ss	42	5.67	nd	Caron, et al. 2011
10 ss	69	5.5	nd	Zhang, et al. 2012
10 ss	50	4.2	nd	Liu, et al. 2011
10 ss	55	4.2	nd	Chen, et al. 2012
10 ss	56	6.3	nd	Lin and Xu, 2009
10 ss	57	5.97	2250	Navis, et al. 2013

*Values were approximated from graphed data if the average was not directly reported.

ss=somite stage

nd=not determined